Escola de Primavera de Transição e Turbulência
Blumenau 2022

ABCM
13th Spring School on Transition and Turbulence
September 19th-23rd, 2022, Blumenau, SC, Brazil

EPTT-2022-0025
CFD STUDY OF TRANSIENT BEHAVIOR OF GAS-LIQUID WAVY-STRATIFIED FLOW THROUGH AN ORIFICE PLATE

Josiane Weise
Emilio E. Paladino
SINMEC/UFSC - Computational Fluid Dynamics Lab, Mechanical Engineering Department, Federal University of Santa Catarina, 88040-900 Florianopolis - SC, Brazil
josiane.weise@gmail.com, emilio.paladino@ufsc.br

Abstract. *The multiphase flow through differential pressure (DP) flow meters has a complex behavior, mainly if large-scale interfaces characterize the upstream flow. In this work, a transient Computational Fluid Dynamic (CFD) study of wavy-stratified gas-liquid flow through an orifice plate is presented. The geometry considered is a 0.5 diameter ratio orifice plate arranged in a 25.4 mm internal diameter horizontal pipe. The Two-Fluid model was employed as the multiphase approach, and the realizable k-ε mixture model was used for turbulence modeling. A hybrid segregated-dispersed drag model was implemented, considering the sudden phase morphology change that occurs with the interaction of the phases with the orifice plate. Results for two air-water flow experimental conditions at atmospheric pressure are discussed. Transient fluctuations of DP and phase distributions were compared with the DP signal and flow images acquired with a High-Speed Camera in an experimental facility designed for this study. The model could represent the propagation of waves in the upstream flow and the positive correlation between the DP fluctuations and the liquid fraction in the gas-liquid mixture. The CFD results provide a detailed fluid dynamics analysis to understand the correlation between the liquid fraction and the DP fluctuations, which is essential for developing the technique that measures the flow rate of both phases from a single measuring DP instrument.*

Keywords: *Gas-liquid flows, orifice plate, differential pressure fluctuations, two fluid model, hybrid drag model*

1. INTRODUCTION

Inline multiphase flow measurement requires the determination of the mass flow rate or phase velocities together with the phase fractions. However, the techniques used to measure the phase fractions could not be sufficiently robust, especially in field applications in the oil and gas industry. Studies focusing on differential pressure (DP) flow meters for high gas volume fraction gas-liquid flows have proposed the determination of phase fractions from their correlation with the transient fluctuations of the DP signal (Wenran and Yunxian, 1995; Xu *et al.*, 2003; Zheng *et al.*, 2016). In this way, it would be possible to determine from a single variable, that is, from the measurement of the transient DP signal, the velocity and the fraction of the phases, providing significant advantages in terms of simplicity, operation, and maintenance costs. Such an approach requires studies to determine how fluid dynamics characteristics of the two-phase flow are related to DP fluctuations. Computational Fluid Dynamic (CFD) models are valuable tools for this study because they can provide details on the transient pressure, velocity, and volumetric fraction fields in the DP flow meter. In addition, from a CFD model, it is possible to evaluate different operational and geometric conditions at a much lower cost when comparing to carry out experiments.

Most CFD studies on high gas volume fraction multiphase flow through DP flow meters were conducted in steady-state simulations. The wet gas flow through a Venturi flow meter was studied by He and Bai (2012) and Jing *et al.* (2019) applying the Discrete Phase model (DPM). The comparison between simulation results and the experimental data was performed from the over-reading parameter (OR). The OR parameter is the ratio between the apparent gas mass flow rate predicted from the multiphase DP through the throttle device and the actual gas mass flow rate. Wang *et al.* (2021) used the mixture multiphase model to simulate the steam-water flow in a Venturi flow meter and showed that the OR increases sharply with the amount of steam. Xu *et al.* (2014) presented a comparison between the DPM model and the Eulerian model for the simulation of wet gas flow through a long-throat Venturi. He *et al.* (2018) simulated the wet gas annular flow through a Cone sensor using the Volume of Fluid (VOF) model coupled with the DPM model. In this study, a comparison between the gas-liquid distribution observed from flow images and results obtained by simulation was presented. Regarding transient simulations, Imada (2014) and Weise *et al.* (2021) performed CFD studies of the wet gas flow through an orifice plate flow meter with the Two-Fluid model. In Weise *et al.* (2021) the authors verified the influence on transient DP fluctuations associated with upstream phase distribution. Zhang *et al.* (2021) also presented a transient CFD study of the gas-liquid flow through an orifice plate. They applied the VOF model and simulated flow conditions with higher liquid content, but DP fluctuations were not evaluated.

Modeling gas-liquid flow with high gas fractions through DP flow meters involves critical aspects. The measuring device can cause abrupt changes in the cross-sectional area of the flow, and different interface scales can be observed across the domain. Considering the orifice plate, if the upstream flow is characterized by a large-scale interface (stratified,

wavy-stratified, or annular flow), the device causes the breakdown of the interface into liquid droplets that are entrained in the gaseous core. The liquid can also form a film on the downstream wall. In these cases, interface tracking or capture methods, such as the Level-Set method (Sethian and Smereka, 2003) or the Volume-of-Fluid (VOF) (Hirt and Nichols, 1981) are not applicable, given the multiplicity of interface scales observed in the flow. An alternative for modeling large and small interface scales in the same domain is the use of closure laws and numerical schemes in the Two-Fluid model capable of dealing with dispersed and segregated flows (Štrubelj and Tiselj, 2011; Marschall, 2011; Höhne and Vallée, 2010; Höhne and Mehlhoop, 2014; Porombka and Höhne, 2015; Mathur *et al.*, 2019).

In this work, we investigate the capability of the Two-Fluid model with a hybrid dispersed-segregated drag model in representing a wavy-stratified gas-liquid flow through an orifice plate, focusing on the relation between the DP fluctuations and the liquid fraction. In this way, the fundamentals of the method that uses only one DP flow meter to evaluate the gas and liquid mass flow rates through the transient DP measurement are investigated.

2. METHODOLOGY

A transient simulation of the gas-liquid two-phase flow through an orifice plate was performed for the present analysis, with the Two-Fluid model combined with a hybrid dispersed-segregated drag model. The URANS (Unsteady Reynolds-averaged Navier–Stokes) approach has been used to evaluate the transient behavior. Considering the Two-Fluid model, the mass and momentum conservation equations for a turbulent flow without mass transfer between phases are, respectively, given by,

$$\frac{\partial}{\partial t}\left(\alpha_k \rho_k\right) + \nabla \cdot \left(\alpha_k \rho_k \mathbf{u}_k\right) = 0, \tag{1}$$

$$\frac{\partial}{\partial t}\left(\alpha_k \rho_k \mathbf{u}_k\right) + \nabla \cdot \left(\alpha_k \rho_k \mathbf{u}_k \mathbf{u}_k\right) = -\alpha_k \nabla P + \nabla \cdot \left[\alpha_k \left(\mathbf{T}_k + \mathbf{T}_k^t\right)\right] + \alpha_k \rho_k \mathbf{g} + \mathbf{M}_{I,k}, \tag{2}$$

where k denotes the phase, α_k is the phase volume fraction, ρ_k, is the phase density, $\mathbf{u}_k$ is the phase velocity, P is the pressure that is shared by both phases. $\mathbf{T}_k$ and $\mathbf{T}_k^t$ are the phase viscous and turbulent stress tensors, respectively, and $\mathbf{M}_{I,k}$ represents the interfacial momentum transfer through the interfaces.

The turbulent stress tensor of each phase is calculated from the turbulent viscosity (μ_k^t), assuming the Boussinesq hypothesis. In this work, turbulent viscosity is calculated according to the realizable $k-\varepsilon$ model, using the mixture multiphase approach. The enhanced wall treatment was applied to modeling turbulence in the near wall regions, which combines a two-layer model with wall functions (Ansys Inc., 2018).

The simulations were performed considering only the drag force in the interfacial momentum transfer. Regarding the phase morphology, two regimes were considered: the dispersed regime of droplets distributed in a continuous gas phase and the segregated regime. So, the interfacial momentum transfer is given by,

$$\mathbf{M}_I = f_s \mathbf{M}_{D,s} + f_d \mathbf{M}_{D,d}, \tag{3}$$

where the weighting function depends on the gradient of the volume fraction as proposed in Porombka and Höhne (2015), such that,

$$f_d = \left[1 + e^{a_d(\alpha_l - \alpha_{lim})}\right]^{-1} \left[1 + c_g |\nabla \alpha_g|\right]^{-1}, \tag{4}$$

$$f_s = 1 - f_d \tag{5}$$

where the model constants were set as $a_d = 50$ and $\alpha_{lim} = 0.3$ as sugested by Porombka and Höhne (2015) and c_g was considered equal to 5×10^{-2} in the orifice plate upstream pipe and 5×10^{-4} in the downstream pipe. The drag in the regions identified as large-scale interfaces is based on the model proposed by Marschall (2011). The expression is written as:

$$\mathbf{M}_{D,S} = \lambda(\mathrm{Re}_I, \pi_\mu) \frac{|\nabla \alpha_g|}{\delta} \frac{\mu_g \mu_l}{\mu_g + \mu_l} \mathbf{u}_r, \tag{6}$$

where $\mathbf{u}_r$ is the relative velocity between phases and $\lambda(\mathrm{Re}_I, \pi_\mu) = m\mathrm{Re}_I + n\pi_\mu$ represents a dimensionless friction coefficient, in which the first term is based on the definition of the interfacial Reynolds number, which in this work is given by

$$\mathrm{Re}_I = \frac{\rho_m \delta |\mathbf{u}_r|}{\mu_g \mu_l / (\mu_g + \mu_l)}. \tag{7}$$

The second term, π_μ was calculated from Eq. (8):

$$\pi_\mu = \frac{\alpha_g \alpha_l \mu_g \mu_l / (\alpha_l \mu_g + \alpha_g \mu_l)}{\mu_g \mu_l / (\mu_g + \mu_l)}. \tag{8}$$

The parameters m and n are model constants, to which the values 0.5 and 8 are assigned, respectively, and δ is the thickness of the interface which is approximated by,

$$\delta = \frac{1}{|\nabla \alpha_g|}. \tag{9}$$

In regions characterized as dispersed liquid, the drag is calculated as follow,

$$\mathbf{M}_{D,d} = \frac{1}{8} C_D A_i \rho_g |\mathbf{u}_r| \mathbf{u}_r, \tag{10}$$

where the C_D is the drag coefficient calculated according to Schiller and Naumann (1935) correlation and A_i is the interfacial area density, which is a function of the droplet diameter (d_l),

$$A_i = \frac{6\alpha_l}{d_l}, \tag{11}$$

wherein d_l was considered equal to 0.5 mm, based on Pan and Hanratty (2002) and Bae *et al.* (2019).

The simulations were carried out for air-water flow. The compressible nature of the air was modeled using the ideal gas law. So, the energy conservation equation was solved for the gas phase, but the viscous dissipation and the interfacial heat transfer have been neglected.

The computational domain consists of the orifice plate and the upstream and downstream pipes, with 25.4 mm internal diameter (D) and lengths of 100 D and 50 D, respectively. The diameter ratio of the orifice plate is 0.5, and the thickness is 3 mm. The computational domain dimensions were based on test section dimensions of an experimental bench designed for the DP acquisition simultaneously with the flow images from a High-Speed Camera. The hexahedral O-grid type mesh has about 1,930,000 elements. The mesh appearance is shown in Fig. 1 in the longitudinal view and at the pipe and the restriction cross-section views. The grid was refined near the pipe walls. Also, the refinement is performed gradually from the domain ends towards the orifice plate in the mean flow direction.

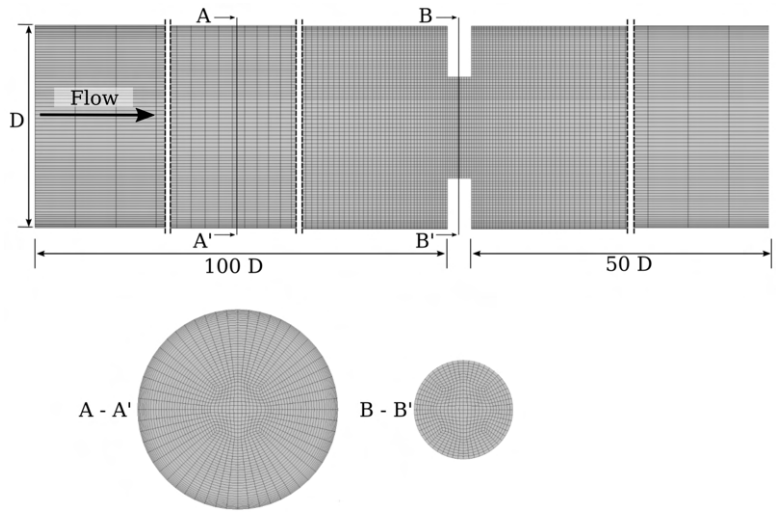

Figure 1. Longitudinal and cross-sections of the computational grid.

Numerical simulations were carried out using the commercial CFD code ANSYS FLUENT 19®, which uses the finite volume method for unstructured grids to solve the governing transport equations. Regarding numerical schemes, volume fraction and velocity were discretized using the modified HRIC scheme and second-order upwind, respectively, and for turbulent properties, first-order upwind was applied. The second-order implicit transient formulation was used with a time-step of 2.5×10^{-5} s. The Phase-Coupled SIMPLE algorithm was applied for pressure–velocity coupling.

Air and water enter separately in the flow domain, setting the mass flow rate of each phase according to the conditions evaluated experimentally. The liquid inlet is performed peripherally while the gas enters from the core region. The gas mass flow rate at the inlet is 0.0063 kg/s in both analyzed flow conditions, resulting in a superficial velocity equal to 10.3 m/s at the outlet (atmospheric pressure). The liquid superficial velocity is 0.065 m/s for Case 1 and 0.1 m/s for

Case 2. Pressure-outlet boundary condition was applied at the outlet (atmospheric pressure), and the non-slip boundary condition was set at the walls for gas and liquid phases. The temperature at the inlet and the walls is considered equal to 20°C. The convergence criterion was set as 10^{-4} for scalable residuals. About 4 s of physical time was used for statistical analysis after a statistically developed regime was observed.

3. RESULTS AND DISCUSSION

In Fig. 2 and Fig. 3 a set of results are presented for the cases with the liquid superficial velocity equals to 0.065 m/s and liquid superficial velocity equals to 0.1 m/s, respectively. The analysis of the results is based on the mass flow rate fluctuations of the liquid phase and DP fluctuations through the restriction. Also, the contours of the gas volume fraction and gas velocity are presented. In Fig. 2 and Fig. 3, images of the flow and the fluctuations of the DP obtained experimentally are also shown for comparison.

The liquid mass flow rate was evaluated in the simulations in a plane positioned perpendicular to the main flow direction focusing in the orifice plate region. In the simulations (point monitors) and in the experiments, the DP was monitored at the bottom of the pipe with a distance of 1 D from the upstream and downstream faces of the orifice plate. The correlation between liquid mass flow fluctuations and DP fluctuations is evident in both cases. In turn, liquid mass flow rate fluctuations are directly related to the propagation of waves through the orifice plate, as can be seen from the contours of the gas volumetric fraction. Proportional fluctuations in the liquid mass flow through the orifice plate were observed related to the amplitude, velocity, and length of the upstream waves. As more liquid is present in the orifice plate, the smaller the area available for the gas flow, and the higher the velocity that the gas phase reaches when passing through the orifice plate. This behavior can be observed from the analysis of volumetric fraction fields in conjunction with the gas velocity field in Fig. 2 and Fig. 3. The blockage in the gas flow area causes abrupt variations in upstream pressure, which result in larger DP fluctuations, in the same way as it was observed in the experiments. Therefore, Fig. 2 and Fig. 3 show the fluid dynamic characteristics that result in the observed relationship between DP fluctuations and the upstream flow structure, which depends on the liquid fraction and it's the main focus of the developed analysis.

Figure 4 shows the structure of the gas phase flow for the case with the liquid superficial velocity of 0.1 m/s at different times during the propagation of a wave through the orifice plate. The time interval between the images is 0.3 s, and the height of the images has been two times enlarged for better viewing. Between t_0 and t_2, it is observed the changes in the gas flow behavior due to the growth of the wave upstream of the restriction, with the formation of a low-velocity region ahead of the wave and high-velocity region over the wave crest. At the time t_3, when the liquid volume at the orifice reduces the gas flow area even more significantly, the deceleration of the upstream gas is observed, and at t_4, the flow of gas is accelerated again, as the area of the orifice occupied by the liquid decreases. In the downstream region, larger recirculation regions are observed predominating in the lower part of the pipe, below the liquid jet, and smaller recirculation regions in the upper part, especially on the edge of the orifice plate. The structure of the downstream flow is constantly modified because of the phases interaction and the dynamics of the liquid jet that forms from the orifice plate.

Regardless of wave formation, it is observed that the orifice plate causes liquid blockage on the upstream face. The dammed liquid tends to be deposited again on the film by the gravity action, joining the liquid main flow, while the liquid closer to the edge of the orifice ends up being dragged by the gas. This interaction between the upstream liquid film and the orifice plate produces variations in the liquid flow through the restriction device and, consequently, DP fluctuations. Therefore, even when there is no formation of characteristic structures in the upstream flow, such as waves or slugs, DP fluctuations can still be correlated with the liquid flow through the orifice plate and with the liquid fraction in the mixture. This result was observed by Weise *et al.* (2021) in the simulation of the wet gas flow through an orifice plate, considering a dispersed phase morphology upstream of the constriction, and better correlation was observed when an annular phase distribution was simulated. Zhang *et al.* (2021) also showed that the water extrusion degree into the air constantly is changed in a stratified flow with higher liquid fractions through an orifice plate. The conclusion was reached based on the downstream jet structure, although the simulations were conducted for a short time after a clear morphology for the jet was detected.

The comparison of gas volume fraction contours with the images obtained from the flow allows the observation that the simulations can capture the wave behavior when it gets closer to the orifice plate. The liquid at the wave crest is dragged with a higher velocity, resulting in the increase of the liquid entrainment in the gaseous core, which is observed in the Fig. 3c) (t_1 and t_2), as in Fig. 3e) (t_2). However, the CFD model does not adequately capture the rupture of the gas-liquid interface in the orifice plate. Therefore, higher dispersion of the liquid phase downstream of the orifice plate is observed in the flow images. It is noteworthy, however, that the analysis of the flow images in the downstream region is more affected by the fact that the entire flow section is captured and not just the flow in the central plane. Thus, all the liquid dragged through the orifice plate is visualized in the flow images, while just the liquid dragged from the lower edge of the restriction is shown in the simulation results. The formation of a liquid film on the pipe walls after the orifice plate observed in the experiments is also observed in simulations, such as exemplified in Fig. 5 from isosurfaces for the gas volume fraction with the isovalue of 0.3 in Fig. 5a) and 0.9 in Fig. 5b).

Comparing the DP results presented for Case 1 and Case 2, both from numerical simulations and experiments, it is

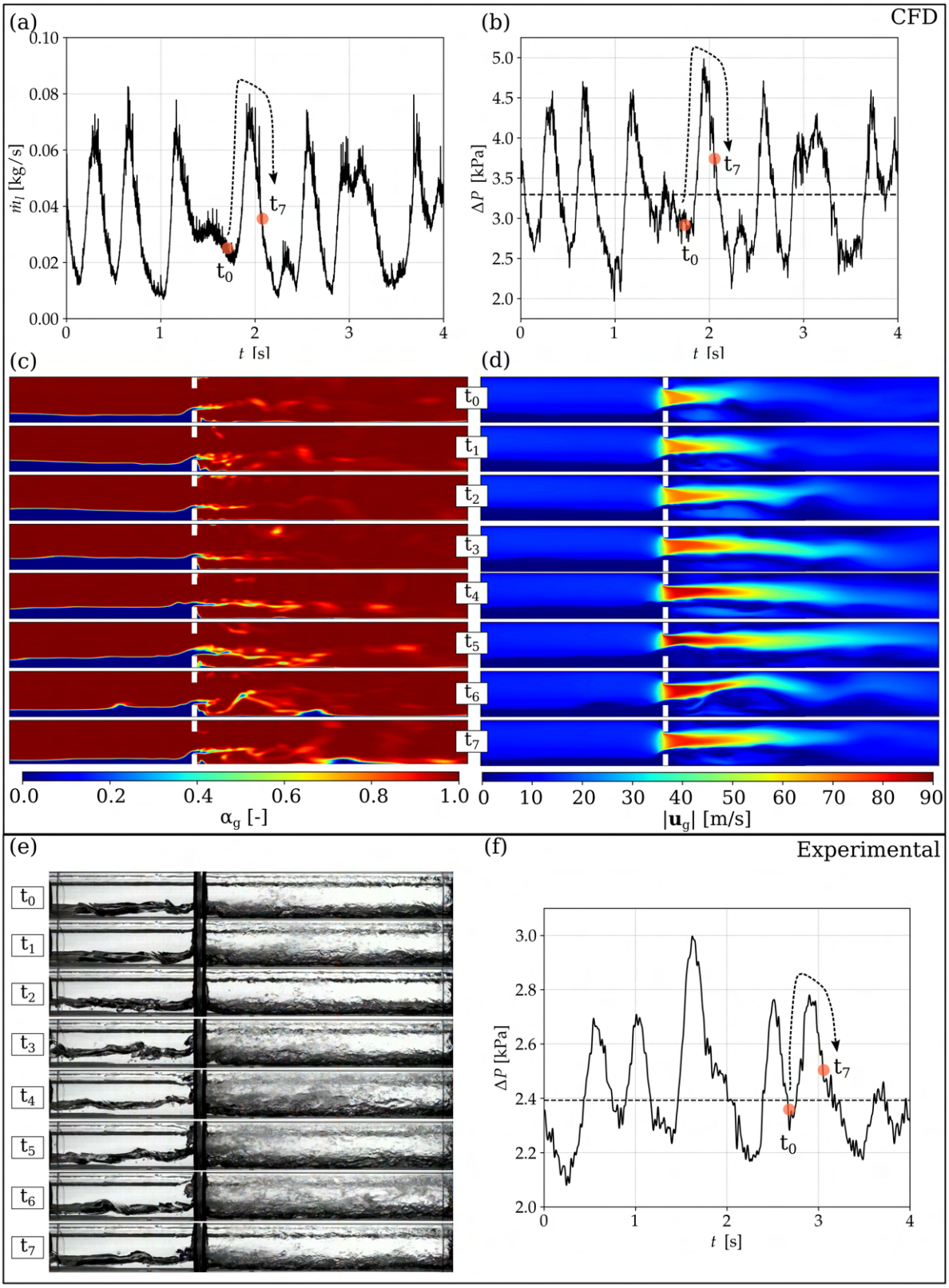

Figure 2. Simulation results for the Case 1 with gas superficial velocity of 10.3 m/s and liquid superficial velocity of 0.065 m/s: (a) liquid mass flow rate fluctuations through the orifice plate; (b) diferential pressure fluctuations through the orifice plate; (c) contours of gas volume fraction at a central plane; (d) contours of gas velocity magnitude at a central plane; (e) HSC flow images; (f) experimental diferential pressure fluctuations. The time interval between images is equal to 50 ms.

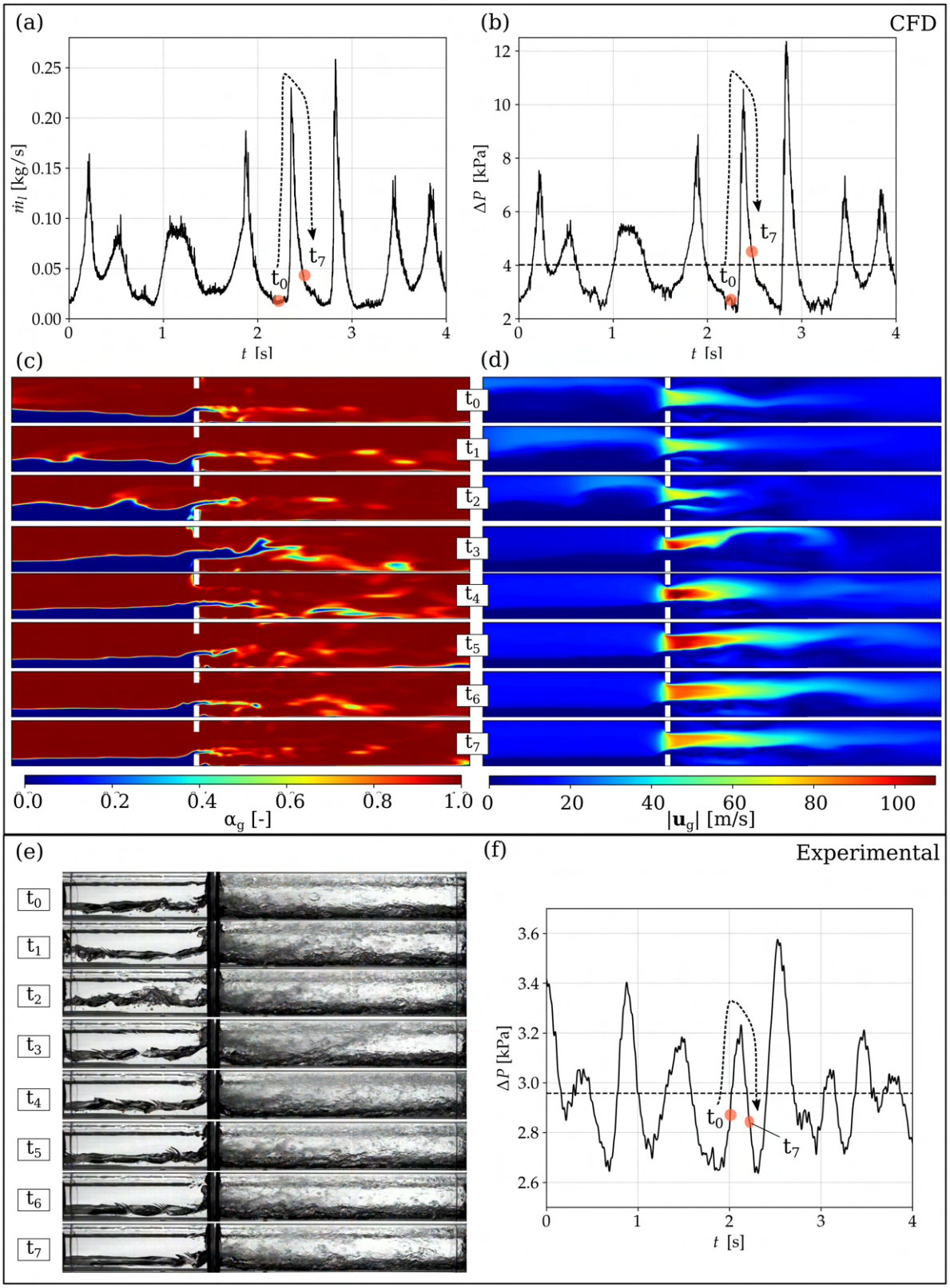

Figure 3. Simulation results for the Case 2 with gas superficial velocity of 10.3 m/s and liquid superficial velocity of 0.1 m/s: (a) liquid mass flow rate fluctuations through the orifice plate; (b) diferential pressure fluctuations through the orifice plate; (c) contours of gas volume fraction at a central plane; (d) contours of gas velocity magnitude at a central plane; (e) HSC flow images; (f) experimental diferential pressure fluctuations. The time interval between images is equal to 30 ms.

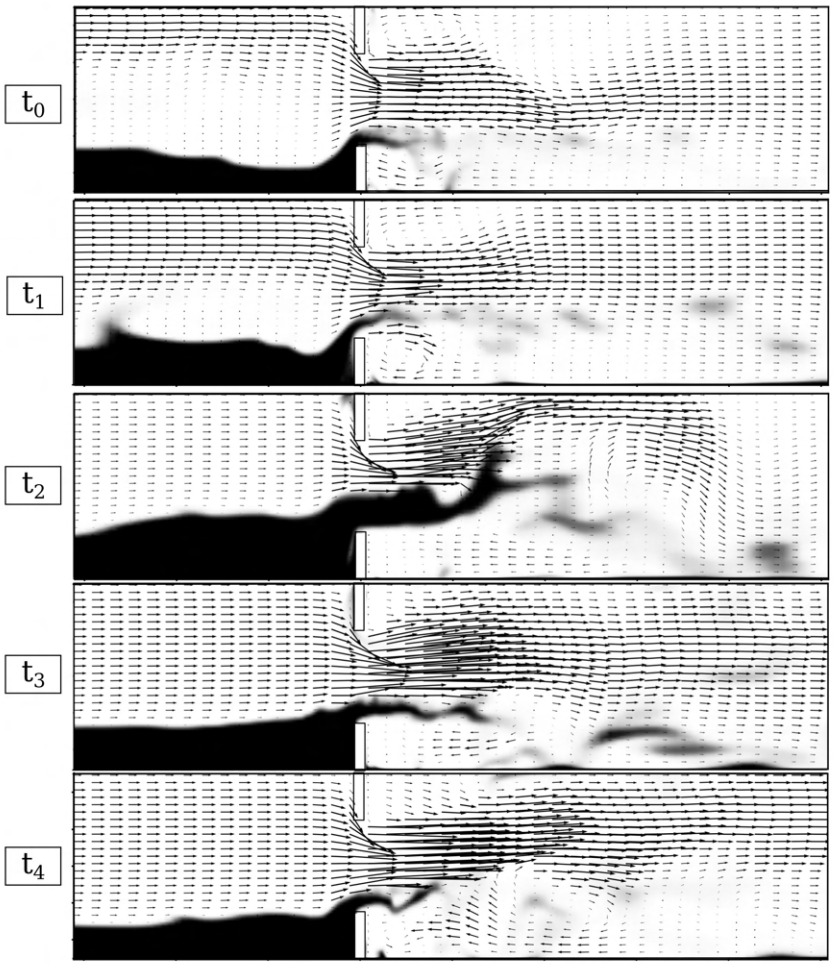

Figure 4. Gas volume fraction and gas velocity vectors instantaneous fields during a wave propagation through the orifice plate. The time interval between images is 0.3 s and in the images the height has been magnified twice for better visualization.

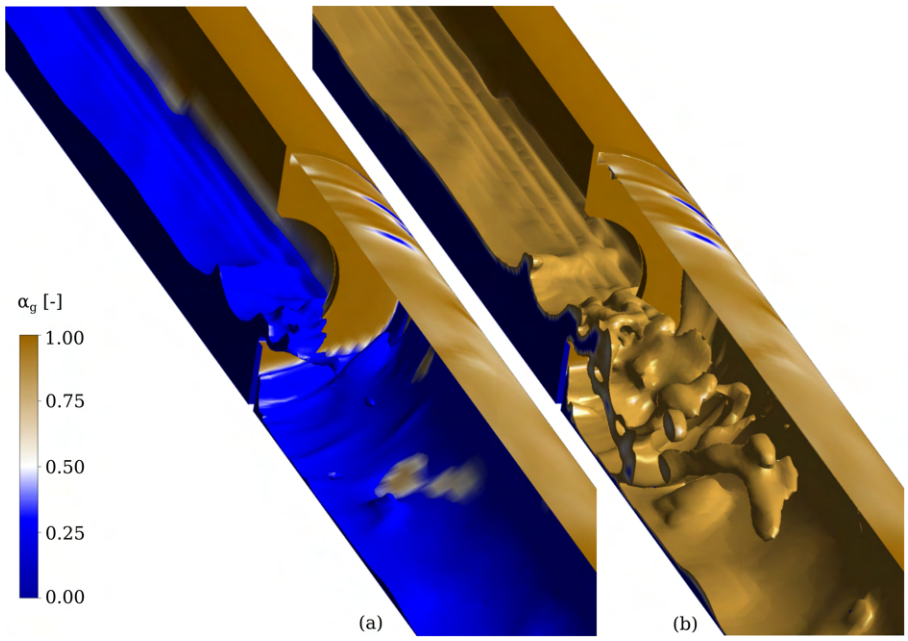

Figure 5. Isosurfaces for the gas volume fraction with the isovalue of (a) 0.3 and (b) 0.9

possible to notice a positive correlation between the liquid fraction with the mean of the DP and the amplitude of the DP fluctuations. So, numerical and experimental results are qualitatively consistent. However, the mean and the standard deviation of the DP are overpredicted by simulations. CFD simulations overpredict the mean of the DP by approximately 36% for both cases. Concerning the standard deviation of the DP fluctuations, the value obtained from the simulation is 3.7 and 6.7 times greater than the experimental result for Cases 1 and 2, respectively. These errors can be related to the model failure in representing the interface rupture as the liquid comes into contact with the orifice plate and the liquid phase behavior as this rupture occurs. Therefore, the peaks of the DP fluctuations in the simulations are higher than in the experiments because the interface does not break up, causing a more significant reduction in the gas flow area at the orifice plate. The point mentioned seems to be the major challenge in modeling the large-scale interface flow through the orifice plate, and further investigations are needed.

4. CONCLUSIONS

In this study, a hybrid model for the drag force was implemented for the transient simulation of a wavy-stratified flow through an orifice plate using the Two-Fluid model. The influence of the liquid superficial velocity on the transient behavior of the flow was evaluated, and the numerical results were compared with experiments through DP fluctuations and High-Speed Camera flow images.

The numerical model can represent the formation of waves upstream of the restriction for the conditions analyzed and qualitatively capture the positive correlation between the mean and standard deviation of the differential pressure through the orifice plate with the liquid fraction in the flow. However, both parameters are overpredicted by the CFD model. Further studies should investigate the process of the interface rupture in the orifice plate and improve the modeling of interfacial transfer terms to better deal with liquid entrainment and liquid dispersion.

5. ACKNOWLEDGEMENTS

The authors would like to thank to Conselho Nacional de Desenvolvimento Científico e Tecnlógico (CNPq, Brazil). Also the authors acknowledge the National Laboratory for Scientific Computing (LNCC/MCTI, Brazil) and Computational Fluid Dynamics Lab (LFC, University of Blumenau) for providing HPC resources, which have contributed to the research results reported within this paper.

6. REFERENCES

Ansys Inc., 2018. *ANSYS Fluent 19.2 Theory Guide*.

Bae, B., Kim, T., Kim, K., Jeong, J.J. and Yun, B., 2019. "Experimental investigation of droplet entrainment and deposition in horizontal stratified wavy flow". *International Journal of Heat and Mass Transfer*, Vol. 144, p. 118613.

He, D. and Bai, B., 2012. "Numerical investigation of wet gas flow in Venturi meter". *Flow Measurement and Instrumentation*, Vol. 28, pp. 1–6.

He, D., Chen, S. and Bai, B., 2018. "Experiment and numerical simulation on gas-liquid annular flow through a cone sensor". *Sensors*, Vol. 18, No. 9, p. 2923.

Hirt, C.W. and Nichols, B.D., 1981. "Volume of fluid (vof) method for the dynamics of free boundaries". *Journal of computational physics*, Vol. 39, No. 1, pp. 201–225.

Höhne, T. and Mehlhoop, J.P., 2014. "Validation of closure models for interfacial drag and turbulence in numerical simulations of horizontal stratified gas-liquid flows". *International Journal of Multiphase Flow*, Vol. 62, pp. 1–16.

Höhne, T. and Vallée, C., 2010. "Experiments and numerical simulations of horizontal two-phase flow regimes using an interfacial area density model". *The Journal of Computational Multiphase Flows*, Vol. 2, No. 3, pp. 131–143.

Imada, F.H.J., 2014. *Estudo da estrutura multidimensional de escoamentos multifásicos em dispostivos de medição de pressão diferencial*. Master's thesis, Universidade de São Paulo, Brazil, São Paulo.

Jing, J., Yuan, Y., Du, S., Yin, X. and Yin, R., 2019. "A cfd study of wet gas metering over-reading model under high pressure". *Flow Measurement and Instrumentation*, Vol. 69, p. 101608.

Marschall, H., 2011. *Towards the numerical simulation of multi-scale two-phase flows*. Ph.D. thesis, Technische Universität München.

Mathur, A., Dovizio, D., Frederix, E. and Komen, E., 2019. "A hybrid dispersed-large interface solver for multi-scale two-phase flow modelling". *Nuclear Engineering and Design*, Vol. 344, pp. 69–82.

Pan, L. and Hanratty, T.J., 2002. "Correlation of entrainment for annular flow in horizontal pipes". *International Journal of Multiphase Flow*, Vol. 28, No. 3, pp. 385–408.

Porombka, P. and Höhne, T., 2015. "Drag and turbulence modelling for free surface flows within the two-fluid euler-euler framework". *Chemical Engineering Science*, Vol. 134, pp. 348–359.

Schiller, L. and Naumann, Z., 1935. "A drag coefficient correlation". *VDI Zeitung*, Vol. 77, pp. 318–320.

Sethian, J.A. and Smereka, P., 2003. "Level set methods for fluid interfaces". *Annual review of fluid mechanics*, Vol. 35,

No. 1, pp. 341–372.

Štrubelj, L. and Tiselj, I., 2011. "Two-fluid model with interface sharpening". *International journal for numerical methods in engineering*, Vol. 85, No. 5, pp. 575–590.

Wang, H., Zhu, Z., Zhang, M. and Han, J., 2021. "Numerical investigation of the large over-reading of venturi flow rate in are of nuclear power plant". *Nuclear Engineering and Technology*, Vol. 53, No. 1, pp. 69–78.

Weise, J., Baliño, J.L. and Paladino, E.E., 2021. "Cfd study of the transient wet gas flow behavior through orifice plate flow meters". *Flow Measurement and Instrumentation*, Vol. 82, p. 102077.

Wenran, W. and Yunxian, T., 1995. "A new method of two-phase flow measurement by orifice plate differential pressure noise". *Flow Measurement and Instrumentation*, Vol. 6, No. 4, pp. 265–270.

Xu, L., Xu, J., Dong, F. and Zhang, T., 2003. "On fluctuation of the dynamic differential pressure signal of Venturi meter for wet gas metering". *Flow Measurement and Instrumentation*, Vol. 14, No. 4-5, pp. 211–217.

Xu, Y., Gao, L., Zhao, Y. and Wang, H., 2014. "Wet gas overreading characteristics of a long-throat Venturi at high pressure based on CFD". *Flow Measurement and Instrumentation*, Vol. 40, pp. 247–255.

Zhang, Y., He, C. and Li, P., 2021. "Numerical investigation of gas-liquid two-phase flow in horizontal pipe with orifice plate". *Progress in Nuclear Energy*, Vol. 138, p. 103801.

Zheng, X., He, D., Yu, Z. and Bai, B., 2016. "Error analysis of gas and liquid flow rates metering method based on differential pressure in wet gas". *Experimental Thermal and Fluid Science*, Vol. 79, pp. 245–253.

7. RESPONSIBILITY NOTICE

The authors are the only responsible for the printed material included in this paper.